Integrated Combined Cycle from Natural Gas with CO_2 Capture Using a Ca–Cu Chemical Loop

Isabel Martínez, Ramon Murillo, and Gemma Grasa
Instituto de Carboquímica, Consejo Superior de Investigaciones Científicas (CSIC), Miguel Luesma Castán 4, Zaragoza 50018 Spain

Jose R. Fernández and Juan Carlos Abanades
Instituto Nacional del Carbón, Consejo Superior de Investigaciones Científicas (CSIC), Francisco Pintado Fe 26, Oviedo 33011 Spain

DOI 10.1002/aic.14054
Published online February 27, 2013 in Wiley Online Library (wileyonlinelibrary.com)

The integration in a natural gas combined cycle (NGCC) of a novel process for H_2 production using a chemical Ca–Cu loop was proposed. This process is based on the sorption-enhanced reforming process for H_2 production from natural gas with a $CaO/CaCO_3$ chemical loop, but including a second Cu/CuO loop to regenerate the Ca-sorbent. An integration of this system into a NGCC was proposed and a full process simulation exercise of different cases was carried out. Optimizing the operating conditions in the Ca–Cu looping process, 8.1% points of efficiency penalty with respect to a state-of-the-art NGCC are obtained with a CO_2 capture efficiency of 90%. It was demonstrated that the new process can yield power generation efficiencies as high as any other emerging and commercial concepts for power generation from NGCC with CO_2 capture, but maintaining competing advantages of process simplification and compact pressurized reactor design inherent to the Ca–Cu looping system. © 2013 American Institute of Chemical Engineers *AIChE J*, 59: 2780–2794, 2013

Keywords: design (process simulation), energy, simulation, process, environmental

Introduction

The recent World Energy Outlook 2011[1] indicates that natural gas (NG) demand will keep increasing its share in the world energy mix over the next two decades, particularly due to its boost in the electricity generation section. In this sector, the state-of-the-art large-scale natural gas combined cycle (NGCC), is a well-established commercial technology due to its high efficiency and reliability with low CO_2 emissions and investment costs. However, NGCC with nearly zero CO_2 emissions is a necessary condition to make the exploitation of the vast reserves of NG compatible with the long-term goals for climate change mitigation.[2]

There are different alternatives to accomplish this scheme of NGCC with nearly zero emissions that imply different grades of modification in the existing combined cycle.[3,4] The first approach proposes carrying out the CO_2 removal from the exhaust gas of a commercial NGCC using chemical absorption by amine solutions.[5–11] This option implies no modifications to the existing gas turbine but for the steam extraction at low pressure (LP) for the stripping section of the capture process and, therefore, is more feasible for the retrofitting of existing power plants. On the basis of this configuration, more compact designs of absorption plants and slightly higher efficiencies result if part of the exhaust flue gas from the gas turbine is recycled to the compressor of the combined cycle after heat recovery, leading to lower investment and operational costs.[5,7,10] A second arrangement is to use a decarbonized fuel into the combined cycle[6,9,12–14] that would require of slightly modifications in the operating parameters of the gas turbine to avoid its malfunctioning. There is a broad range of precombustion processes able to provide a H_2-based fuel to be burnt in the gas turbine, which has been explained in further detail later. Finally, there would be a third alternative route of CO_2 capture in NGCC that proposes using O_2 as oxidizing agent in the combustion chamber of the gas turbine and, therefore, obtaining an exhaust gas consisting mainly of CO_2 and H_2O,[5,6,10,13,15] similar to that in oxy-combustion processes. This option requires redesigning the gas turbine to use CO_2 as working fluid and also including an air separation unit (ASU), which would greatly increase the cost and negatively affect the efficiency. In this oxy-combustion context and to avoid including the ASU, different process configurations have been proposed such as the advanced zero emission plant,[11,13] or the integration of either a solid oxide fuel cell[11,16,17] or chemical looping combustion process[11,18,19] into a combined cycle. Despite the fact that these options have been reported to have greatly high efficiencies at low CO_2 emissions, none of these options seem likely to be developed in a foreseeable future due to the requirement of challenging either materials or layouts to operate under conditions of conventional gas turbines.

The postcombustion option referred earlier for NGCC with nearly zero CO_2 emissions has been usually adopted as the reference case for power plants from NG including

Correspondence concerning this article should be addressed to I. Martínez at imartinez@icb.csic.es.

carbon capture. The selection of a NGCC equipped with postcombustion CO_2 capture using amines (usually monoethanolamine, MEA) is driven by its simple configuration without modifying the gas turbine operation while relies on more mature technology than other capture options, such as the precombustion routes.[20] The variability of the NGCC net plant efficiency reported in the literature (that could range between 55 and 59%) has led to consider the efficiency penalty to compare the different capture options to the reference NGCC chosen. It has been reported in the literature that this postcombustion CO_2 capture option in NGCC results in an efficiency penalty in the range of 7–10% points when using MEA with a regeneration energy close to 4 GJ/ton CO_2.[4,8–11,21–23] Simulation results point out that as low as 5.5 points of efficiency penalty would result when using a diethanolamine (DEA) absorption system to perform the CO_2 capture in a NGCC,[7] due to its very low energy requirements during regeneration. However, efficiency penalty is not the only criteria to choose among these absorption CO_2 capture options. Although lower regeneration energies are required when using DEA or blended MEA–*N*-methyldiethanolamine (MDEA) solvents, poorer CO_2 performance results from using them due to their low CO_2 absorption rate and, therefore, an absorber height for blended MEA–MDEA of more than three times that with MEA would be required for the same CO_2 capture efficiency.[24] Added to the higher investment costs linked to the usage of blended MDEA or DEA solutions, the stringent requirements of SO_2 and NO_2 acid gases concentrations to avoid heat stable salts formation[25] lead to consider a highly effective gas cleaning system to avoid deteriorating amine, and then incrementing also capital investment. In addition, from an environmental point of view, it is important to consider that amines, but especially MEA, undergo degradation within the process and form ammonia and other toxic degradation products that should be controlled to avoid harmful emissions to the atmosphere.[26] Finally, hazardous solid waste products derived from the recovery of spent solvent should be properly managed to reduce their risks and impacts to the humans and the environment.[27] As a result, all this preventing issues contribute to increase the cost of this CO_2 postcombustion capture process and make other zero emission alternatives gain importance.

Looking through the challenges of the different options mentioned earlier for reducing CO_2 emissions in NGCC, precombustion CO_2 capture in NGCC has received a lot of attention in the last decades as a nearly zero emission alternative.[13] This option comprises the coupling of a commercial chemical process that generates a H_2/CO_2 mixture from NG, which CO_2 concentration is in the range of 15–60% (dry basis) and should be removed to obtain a low-carbon gas stream, and a rich-H_2-fuelled gas turbine. Regardless of the H_2 production process from NG, and due to the fact that growing attention is paid to the possibility of burning H_2 in a gas turbine to reduce CO_2 emissions, heavy duty conventional gas turbines designed to run on NG have to be adapted to be H_2 fuelled until new specific designs to run exclusively on H_2 will be available. Switching from NG to H_2 in a gas turbine leads to consider different operation strategies for adapting the original machine to operate properly, because of the effects of variation of volume flow rates and thermophysical properties of the new fuel.[28] General Electric (GE) turbines, specially 9FB model, allow burning fuels containing up to 60% of H_2 without major changes.[29] These changes would comprise first, decreasing the combustor outlet temperature and the first rotor total inlet temperature (TIT) to avoid excessive metal operating temperature and enlarge component lifetime and, second, closing partially the compressor variable guide vanes (VGV) for reducing the air mass flow while maintaining pressure ratio.[28] By means of these slight modifications, the efficiency of the combined cycle fuelled by H_2 has proven to be similar to that of a conventional NGCC, while gas turbine power output even increases derived from thermodynamic properties of the gas expanded.[28]

Regarding to the H_2 production island, there is a wide variety of existing and commonly used synthesis gas production processes. These processes comprise steam methane reforming (SMR), autothermal reforming (ATR), and partial oxidation (POX).[13] All these technologies have been proposed to be integrated into a combined cycle carrying out an assessment of the efficiency derived.[4,6,11,30–34] These processes usually imply three stages in the fuel processing sequence: (1) primary feedstock conversion into a H_2/CO mixture at high temperature, (2) water–gas shift reaction at intermediate temperature to convert CO to CO_2 and increase H_2 yield, and (3) removal of CO_2 at ambient temperature by means of chemical absorption. A common feature of the integration of these technologies with a combined cycle is to provide the steam required for reforming from a medium pressure bleed of the steam cycle, which translates into a penalty to the process efficiency. Other operating parameters and/or process considerations, such as temperature and pressure of the reforming stage, the amount of air derived from air compressor to the ATR or POX processes, or the physical and chemical absorption/desorption properties of the amine solvent chosen, are also decisive to the efficiency penalty assessed. Under the same combined cycle assumptions and chemical absorption column assumptions using DEA–water solution, plant configuration based on SMR shows poorer performance than that based on POX with respect to a combined cycle of the same technology (10% points of efficiency penalty for SMR vs. 7.6% points for POX[31,32]), mainly due to the fact that steam-to-carbon ratio, S/C, in SMR is extensively higher than in POX. With respect to ATR-based configurations, efficiency penalties when integrating with a combined cycle range from 8% points, when moderate operating conditions and energy requirements are assumed, to 14% points for stringent conditions.[6,11,30,33,34] In view of this published results, POX-based configurations focused on power production by H_2-fuelled gas turbines bring out as those with the best performance together with ATR configurations operating mainly with moderate S/C and energy consumptions in the amine regeneration column.

In addition to the previous set of commercial technology options available for precombustion of NG, novel combined reaction/separation systems have emerged as novel routes of precombustion CO_2 capture to produce H_2, which bring down not only the steam and energy requirements but also the complexity and efficiency decay of the precombustion decarbonization routes aforementioned. The sorption-enhanced reforming (SER), concept proposes integrating a CO_2-acceptor sorbent to enhance H_2 production while reducing catalyst use and leading to process simplification and cost reduction.[35] SER was originally proposed to be carried out in fluidized bed reactors under atmospheric pressure by using Ca-sorbents as CO_2-acceptors.[36,37] However, when

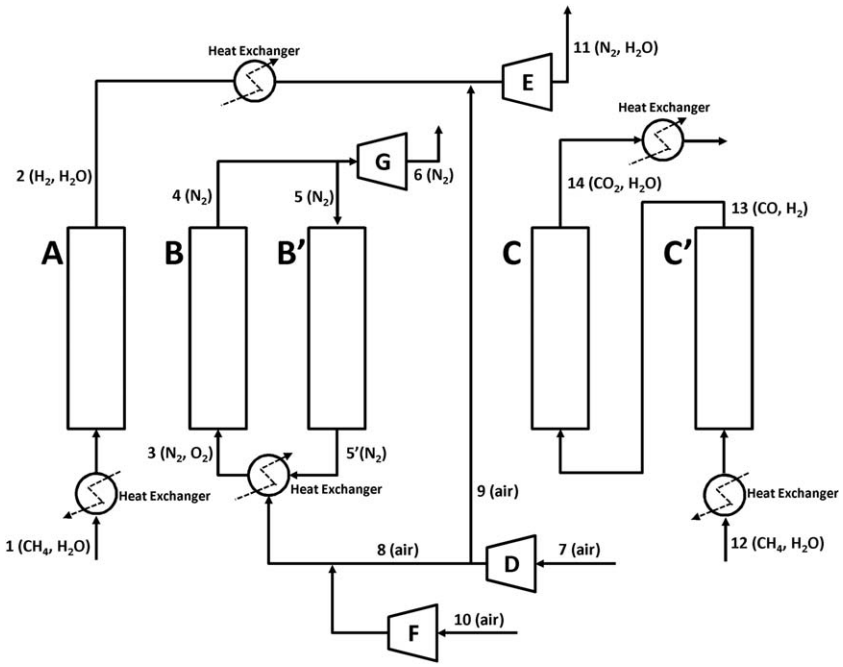

Figure 1. Process layout of the Ca–Cu chemical loop process focused on power generation (based on the scheme proposed by Fernández et al.[48]

D and E are the compressor and the gas turbine of the combined cycle, respectively. F is the external air compressor and G the N_2 expander.

focused on electricity generation by burning rich-H_2 gas in a gas turbine, the higher pressures required lead to either extremely high regeneration temperatures in a rich-CO_2 atmosphere, or lower temperatures when adding steam and/or using other sorbents.[38–40] These sorbent regeneration problems are largely absent operating at lower temperatures than in the sorption-enhanced reaction process. A simplification of this process is the sorption-enhanced water–gas shift (SEWGS) process[41] that maintains the need of a steam reforming step to produce a H_2/CO mixture and integrates in one step the water–gas shift and CO_2 removal. The overall SEWGS process has been shown to result in efficiency penalties from 7 to 9% points when integrating with a combined cycle.[42,43]

An alternative reforming process using CaO as a CO_2 sorbent has been also published by GE whose aim is to solve the problem of the energy needed for sorbent regeneration.[44–46] This process, called unmixed reforming (UMR), was originally proposed for small-scale H_2 production by alternately cycling fuel and air to a packed bed, and is based on including a metal oxygen carrier (usually Ni) into the process together with the CO_2 sorbent. In this way, the energy released in the oxidation of the metal with air is used to regenerate the CO_2 sorbent in the same solid bed and, therefore, an efficient energy transfer occurs and so the energy efficiency increases. However, UMR does not include CO_2 capture since oxidation and sorbent regeneration take place in the same stage, and CO_2 is released diluted with the N_2 from the air.

Based on the UMR but solving the issue of CO_2 emissions, the novel route for H_2 production on which this work is based emerged. The novelty of this process is that the energy for regenerating the CO_2 sorbent is supplied by the exothermic reduction of CuO with NG, CO, or H_2, which takes place in the same solid bed,[47,48] and a rich-CO_2 stream with readily separable H_2O is produced. As this process combines the $CaO/CaCO_3$ and Cu/CuO chemical loops, it gathers the main advantages of the SER and the UMR processes: production of rich-H_2 in one step that leads to a simplified process, no need of an ASU, improved heat transfer, low-cost reactor materials due to the lower temperatures needed, and better heat integration, and so process efficiency.

The main objective of this article is to develop a feasible integration of this novel precombustion route for H_2 production into a NGCC for electricity production, and to carry out an assessment of the net plant efficiency obtained when modifying its operating conditions looking for either high efficiency and/or high CO_2 capture. Finally, the results obtained in this work are compared with the results reported in the literature for other precombustion decarbonization routes integrated into a NGCC.

Process Description

H_2 production island

The process analyzed in this work, briefly outlined in Figure 1, was first proposed by Abanades and Murillo[49] and further described by Abanades et al. [47] For NG precombustion applications, it is proposed to be carried out in fixed-bed reactors, where pressure and temperature can be independently modified to fit the performance requirements needed to obtain a rich-H_2 gas stream from CH_4. Although this process can be designed to produce H_2 and/or electricity, it has been considered in this work the last option and, therefore, the layout proposed by Fernández et al. [48] has been slightly modified to be consistent with this electricity production aim. To be able to produce power, the precombustion CO_2 capture process must be integrated into an advanced combined cycle, based on a heavy duty gas turbine whose operating parameters should be modified to be fuelled with a H_2-enriched fuel instead of NG. Reactions occurring in each

stage and equations used to solve mass and energy balances, as well as the considerations taken into account to decide about operating conditions in each stage, have been widely discussed by Fernández et al.,[48] and, therefore, a brief description is done in this work mainly focused on the energy management in the process.

First step in the process (Stage A in Figure 1) involves H_2 production via SER from CH_4 with steam in the presence of CaO, a Cu-supported material and a certain fraction of a commercial Ni-based reforming catalyst. A catalyst-to-sorbent mass ratio of 0.3 has been maintained constant in every case studied in this work, whereas the amount of Cu-supported material has been adjusted in each case to fulfill the energy balance of the process. Reforming, water–gas shift and carbonation reactions taking place in the fixed-bed reactor, Eqs. 1–3, have been considered to be fast enough to achieve equilibrium at the working conditions. Space velocities typical of the conventional steam reforming (over 4000 Nm^3 CH_4/m^3 cat/h and 0.5 m/s of superficial gas velocity) have been considered. The low superficial velocity of gas chosen in Stage A allows having a negligible pressure drop in this stage of around 2 kPa.

$$CH_4(g)+H_2O(g) \leftrightarrow CO(g)+3H_2(g) \quad \Delta H_{298\,K}=+206\,kJ/mol \tag{1}$$

$$CO(g)+H_2O(g) \leftrightarrow CO_2(g)+H_2(g) \quad \Delta H_{298\,K}=-41\,kJ/mol \tag{2}$$

$$CaO(s)+CO_2(g) \leftrightarrow CaCO_3(s) \quad \Delta H_{298\,K}=-178.8\,kJ/mol \tag{3}$$

As a result of the combined reactions (1)–(3) being thermally neutral in the reactor, temperature in Stage A will not affect significantly the H_2 yield as long as carbonation reaction is favored.[50] However, from a thermal efficiency point of view, the lower the temperature in Stage A, the lower the energy penalty associated with the preheating of the CH_4/steam mixture fed into the SER, and, therefore, an operating temperature of 650°C has been chosen in this stage. The rich-H_2 gas from this stage (Stream 2 in Figure 1) needs to be cooled down and diluted with compressed air to be burnt into the combustion chamber of a state-of-the-art gas turbine, as described in the next section. As design specifications of the gas turbine modeled (parameters based on a GE 9FB gas turbine) imply working with a pressure ratio of around 18.3 in the air compressor and with a fuel overpressure in the combustion chamber of around 20%,[34] with respect to the oxidant stream, operating pressure in Stage A has been considered to be equal to 2200 kPa. Concerning to the S/C molar ratio in SER, higher values tend to enhance CH_4 conversion and H_2 yield. S/C ratios in the range of 3–5 are common in this process,[35] contributing also to minimize coke formation[51] and the subsequent catalyst deactivation. As a result of the S/C molar ratio chosen, a rich-H_2 product gas with a H_2 concentration ranging from 50 to 65% vol. is obtained. This fuel composition, with a great amount of steam, will have a positive effect on NO_x emissions due to the use of steam as dilution agent for reducing NO_x formation in the combustion chamber.[28]

Once the breakthrough of the SER has concluded (end of Stage A), a new reaction stage begins in the fixed bed when diluted air is fed to oxidize Cu and produce the necessary amount of CuO to carry out the subsequent calcination of the $CaCO_3$ formed in Stage A. The oxidation of Cu (Eq. 4) is highly exothermic, and, therefore, this step is one of the main energy outputs from the system.

$$Cu(s)+{}^1/_2O_2(g) \leftrightarrow CuO(s) \quad \Delta H_{298K}=-156.1kJ/mol \tag{4}$$

The evolution of the reaction and heat-exchange fronts in the fixed-bed reactor during Stage B will determine the temperature of the exiting gas (Stream 4). Two different periods of time can be identified: a first period where the gas leaving this stage has the same temperature as the maximum temperature reached during Stage A ($T_{max,A}$ that is between 675 and 695°C). A second period of time exists when the gas stream is at the maximum temperature in Stage B ($T_{max,B}$ between 830 and 870°C). Part of this second gas stream at $T_{max,B}$ is sent to an expander (Unit G in Figure 1) to generate extra power and maximize the net efficiency of the process. After this expansion, this O_2-depleted gas (Stream 6) will be at low temperature around 340–365°C (depending on $T_{max,B}$), suitable to be further cooled down before being sent to the stack. The proportion of gas at $T_{max,A}$ and $T_{max,B}$ leaving Stage B can be adjusted by modifying the proportion of gas recirculated, as it was explained in detail by Fernández et al.[48]

As part of Stream 4 leaving this Stage B at around 1780 kPa (a pressure drop around 50 kPa resulted in this stage from the conditions chosen) is proposed to be used to drive an additional expander and produce power, the oxidation in reactor B needs to be carried out at the maximum allowable temperature. However, very high temperatures are not feasible, because Cu and CaO active surface could be irreversibly lost and an undesired level of $CaCO_3$ calcination could take place. Reasonable values of $T_{max,B}$ considered in this work are in the range of 830–870°C. Fast oxidation kinetics have been reported in the literature[52] at this temperature range even with a low content of O_2 in Stream 3. To moderate the maximum temperature that could be reached in this reactor, oxidation rate should be controlled by reducing the O_2 concentration in the gas fed into Stage B, and simultaneously working with low temperatures in this inlet gas (at 150°C). Under these circumstances of high pressure (HP) and limited temperature, and according to equilibrium calculations, CO_2 concentration at the exit of Stage B will be kept to a minimum of 1.5–3% vol. Such a high dilution of O_2 at the inlet of Stage B will be achieved by recycling a large fraction of the O_2-depleted flue gas exiting this stage (Stream 5) and mixing with compressed air extracted from the compressor of the gas turbine (Stream 8) and from an additional air compressor (Stream 10).

When Stage B finishes, the solid bed is left downstream at the temperature of the gas fed (150°C). This makes impossible to initiate the reduction of CuO with CH_4, CO, or H_2 and the simultaneous $CaCO_3$ calcination (Stage C). Then, it is necessary to introduce an intermediate stage between Stages B and C for raising this bed temperature up to a higher value that allows $CaCO_3$ calcination and reduction of CuO to Cu to take place. Therefore, an additional heat-exchange stage needs to be included (Stage B′) to transfer the excess heat of recycled diluted air to the fixed-bed reactor of depleted Cu.

The recirculation ratio (defined as Stream 5/Stream 4) has been set in 0.85 to minimize efficiency losses, which results

in superficial gas velocities of around 2 m/s. Under these conditions, Stream 5 is not able to raise bed temperature up to $T_{max,B,}$ and, therefore, at the end of this stage, the reactor is left divided into two zones at different temperatures ($T_{max,A}$ and $T_{max,B}$). In any case, part of the flue gas leaving Stage B′ (Stream 5′) is at $T_{max,A}$, which is not cold enough to be introduced again into Stage B at 150°C, and, therefore, an additional heat exchanger is required to remove the energy excess of this stream and that of the compressed air coming from the compressors D and F in Figure 1 at a temperature of around 420°C.

The next step in the process is the $CaCO_3$ calcination by means of the reduction of CuO formed in Stage B. As this stage has been designed to be thermally neutral, the Cu/CaO molar ratio in the solid should be properly chosen to be sure that the heat released in the reaction front by the exothermic reaction of CuO with CH_4, CO, or H_2 is equivalent to the energy required to the endothermic calcination of the $CaCO_3$ formed in Stage A. As it was demonstrated by Fernández et al.,[48] taking into account the energy released in the reduction reactions of CuO with CH_4 (Eq. 5), CO (Eq. 6), and H_2 (Eq. 7), lower values of the Cu/CaO molar ratio were obtained when reducing CuO using syngas. Values ranging from 1.3 to 1.9 were obtained depending on the H_2/CO ratio.

$$4CuO(s)+CH_4(g) \leftrightarrow 4Cu(s)+CO_2(g)+2H_2O(g) \quad \Delta H_{298\,K}=-195.3\,kJ/mol \tag{5}$$

$$CuO(s)+CO(g) \leftrightarrow Cu(s)+CO_2(g) \quad \Delta H_{298\,K}=-131.9\,kJ/mol \tag{6}$$

$$CuO(s)+H_2(g) \leftrightarrow Cu(s)+H_2O(g) \quad \Delta H_{298\,K}=-89.6\,kJ/mol \tag{7}$$

From 700°C onward, reduction kinetics of CuO with H_2 and CO are fast enough to be completed in short times, and, therefore, CuO reduction is not going to be the limiting factor to the operating conditions in Stage C, but the $CaCO_3$ calcination. To have a reasonable temperature in Stage C of around 850–870°C, and then to avoid that Cu- and Ca-based sorbents could sinter and lose their activity, pressure in Stage C must decrease to atmospheric pressure. The operating temperature of Stage C is a variable to study in this work, as it determines the recoverable heat in the rich-CO_2 gas obtained (Stream 14) before being sent to the compression and purification unit (CPU).

Due to the fact that solids in Stage C are left in the bed at the high calcination temperature and to the need of reducing the solid bed temperature down to values of 650°C to start a new cycle, Fernández et al.[48] proposed an additional steam reforming (Stage C′) at atmospheric pressure that provides the syngas fed into Stage C while the solid bed is cooled down to an appropriate temperature. LP steam introduced in Stage C′ is bled from the steam turbine at around 170 kPa, to compensate for the pressure drop in Stages C and C′, which is around 70 kPa for the gas velocity of 10 m/s considered.[48] The S/C ratio of the mixture fed to Stage C′ must be kept low to avoid CO_2 production that could partially carbonate the CaO, and then, reducing the CaO available for the following Stage A. To reduce the calcination temperature from 870 to 850°C, S/C molar ratio in Stage C′ has to be increased to reduce CO_2 partial pressure in Stage C. It has been calculated that S/C ratio in Stage C′ should be increased from 1.5 to 2, when calcination temperature is reduced from 870 to 850°C and, at the same time, the Cu/CaO molar ratio is reduced.

Throughout the process description, it has been highlighted the existence of six different hot streams that need to be cooled down providing valuable heat suitable to be integrated into the process: rich-H_2 gas leaving Stage A (Stream 2), O_2-depleted gas after expansion (Stream 6), O_2-depleted gas leaving Stage B′ (Stream 5′), compressed air from gas turbine compressor and booster compressor before being fed to Stage B (sum of Streams 8 and 10), rich-CO_2 gas leaving Stage C (Stream 14), and exhaust gas of the gas turbine (Stream 11). The energy available in these six hot streams is more than six times the energy required to preheat the gas streams that have to be introduced in the system (gas inlets into Stages A and C′ at 650°C). Due to the large energy availability of the process gas streams, a heat-exchange network has been designed, as described in "Heat-Exchange Network Design" section to accommodate the inputs up to the specifications of each stage and to produce HP, steam to be introduced in the steam cycle, and achieve in this way high power generation and/or CO_2 capture efficiencies.

Power island

Reference Combined Cycle. The technology that represents the state-of-the art of large-scale power plants from NG is the NGCC, due to its high fuel-to-electricity efficiency and its reliability at low CO_2 emissions and investment cost. This power plant has been taken as a reference to be integrated with the Ca–Cu looping system described earlier. A simulation model for a state-of-the-art NGCC has been developed in Aspen Hysys, based on a simple design for the gas turbine section. The specifications for the gas turbine have been adapted from those provided by Romano et al.[34] for a GE 9FB heavy duty gas turbine. The steam cycle has been modeled based on a triple-pressure reheat heat recovery steam generator (HRSG), as it leads to the highest net plant efficiency for a NGCC.[53] Main parameters and model assumptions considered for this reference plant are compiled in Table 1. Part of the air compressor discharge is bled and channeled into the gas turbine initial stages for blade cooling. Coolant flow has been estimated to accomplish the required temperature at the combustor outlet of 1454°C, and it is staged along the first two expansion stages of the gas turbine to fulfill the turbine inlet of 1360°C. After cooling, this air is reintroduced into the gas stream to minimize the impact on turbine performance. NG is fed to the combustor of the gas turbine at 156°C, with a fuel overpressure of 20% with respect to the compressed air. Heat losses of 0.11% of the fuel input have been considered at the combustor.[34] In the modeled HRSG, an intermediate pressure of 2200 kPa has been chosen to match the steam requirement pressure of the reforming step of the Ca–Cu looping process. From this simulation model, a NGCC efficiency of 58.8% has been obtained while CO_2 emissions are 351.3 gCO_2/(kW h).

Integrated Combined Cycle with the Ca–Cu Looping Process. Switching from NG to a H_2-fuelled mode requires from slight modifications in the operating parameters of the modeled reference gas turbine described earlier. The larger steam content in the flue gas when burning a rich-H_2 fuel leads to a higher blade metal operating temperature, and, therefore, a lower turbine inlet temperature (TIT) is needed

Table 1. Main Assumptions for the Reference NGCC Plant Without CO_2 Capture (Taken from Romano et al.[34])

Natural gas	
Composition (% vol.)	82.9% CH_4; 7.8% C_2H_6; 1.8% C_3H_8; 0.8% C_4H_{10}; 1.1% CO_2; 5.5% N_2; 0.1% He
LHV	44.13 MJ/kg
Gas turbine	
Temperature of fuel to combustor	156°C
Pressure ratio	18.3
Compressor polytropic efficiency	91.50%
Compressor outlet temperature	419°C
Combustor outlet temperature	1454°C
TIT	1360°C
Heat losses at combustor	0.11% of fuel input (LHV)
Exhaust gas turbine pressure	104 kPa
Auxiliaries consumption	0.35% of net power
Mechanical efficiency	99.60%
Generator efficiency	98.50%
Steam cycle	
SH/RH temperature	565°C/566°C
Evaporation pressures	12,500/2200/400 kPa
Condensing pressure	4.8 kPa
HP/IP/LP isentropic efficiencies	92/94/88%
Pumps adiabatic efficiencies	70%
Electric efficiency	98.10%
Pressure losses	
HRSG gas side	3 kPa
Temperature differences in HRSG	
Gas–steam	25°C
Gas–liquid	10°C
Pinch point gas-boiling liquid	10°C

Table 2. Summary of the Assumptions Added or Modified in the Integrated Combined Cycle with the Ca–Cu Looping Process

Gas turbine	
Temperature of fuel to combustor	300°C
Percentage of air derived from compressor	12%
TIT	1345°C
Combustor outlet temperature	1433°C
Temperature differences in heat exchangers	
Gas–gas	25°C
Gas-boiling or liquid phase	10°C
Liquid–liquid	10°C
Condensing-liquid	3°C
Booster compressor and fan	
Polytropic efficiency	89%
Mechanical-electric efficiency	96%
Expander	
Polytropic efficiency	80%
Mechanical-electric efficiency	98.1%
Pumps	
Adiabatic efficiency	75%
Mechanical-electric efficiency	92%
CO_2 compressor	
Number of intercooled stages	5
Intercooling temperature	30°C
Intercooling pressure loss	1%
Outlet pressure after compression stages	9000 kPa
Liquid CO_2 final pressure	15,000 kPa
Polytropic efficiency for compressor stages	82%
Pump efficiency	75%
Mechanical-electric efficiency	94%

to enlarge component lifetime. In this case, and according to the calculations made by Romano et al.,[34] it has been assumed for the H_2-fuelled mode calculations a TIT of 1345°C and a reduced combustor outlet temperature of around 1433°C. Additionally, the design pressure ratio of 18.3 has been maintained constant with an inlet air flow reduced by the VGV of the compressor.[28] Moreover, it has been assumed that the rich-H_2 fuel (Stream 2 in Figure 1) has to be cooled down to 300°C to be fed into the combustion chamber of the gas turbine.

As mentioned in the "H_2 production island" section, O_2 needed in Stage B is supplied by introducing compressed air blown from the gas turbine compressor. If too much air is derived to the process from the gas turbine compressor prior to the combustion chamber, the performance and temperature profile of the gas turbine will be dramatically affected. According to the values reported in the literature,[6,33,34] the maximum percentage of air from the compressor gas turbine that can be sent to the precombustion process should be in the range of 12–13%. Due to the fact that the air derived from the air compressor to Stage B in the Ca–Cu looping system represents between 18 and 20%, an external air compressor (Unit F in Figure 1) is required to not affect negatively gas turbine performance. Characteristics assumed for this booster compressor as well as modifications made for the gas turbine from the reference NGCC to be fuelled by rich-H_2 are compiled in Table 2. Additionally, a fan (not depicted in Figure 1 for the sake of simplicity) needs to be included to adequate pressure of recycled gas (Stream 5′) fed into Stage B up to 1830 kPa. Due to the high superficial gas velocity of 2 m/s assumed for the N_2-enriched air fed to Stage B, a pressure drop of around 50 kPa results from passing this gas through the oxidation stage. As part of the gas that leaves Stage B is recycled to Stage B′ for bed heating, a total pressure increase of 100 kPa needs to be transferred to Stream 5′ before being fed to Stage B. Characteristics of this fan have been assumed the same as the booster air compressor, compiled in Table 2.

As indicated previously, for a conventional NGCC plant, the highest net plant efficiency is achieved with a triple-pressure reheat steam cycle configuration.[53] However, a specific design of the HRSG is required in this case, because a significant amount of HP steam could be externally produced to the HRSG thanks to the heat recovered from cooling other process streams. To carry out the design of the steam cycle implemented in this work, and to decide the most favorable configuration for the HRSG, the composite curve (temperature vs. heat recovered/introduced in each stage) of the hot heat source (exhaust gas from the gas turbine) and that of steam were drawn to locate the pinch point between them.[54] Process design was carried out to produce HP-saturated steam external to the HRSG (at 12,500 kPa and 327°C) using available gas streams at high temperature. Therefore, feedwater at conditions similar to those at the LP steam turbine outlet is transferred to an external economizer and evaporator, and then saturated HP steam produced is transferred to the superheater (SH) of the HRSG. To determine the best configuration for the HRSG, an exhaust gas with properties similar to that obtained for a H_2-fuelled gas turbine case was considered. A double-pressure reheat (12,500 kPa and 2200 kPa, to match the operating pressure of Stage A in the Ca–Cu looping process) and a triple-pressure reheat (12,500, 2200, and 400 kPa) configurations have been compared here, as the single-pressure system cannot yield as high efficiency as these configurations.[53] By assuming the same amount of saturated HP steam external to the HRSG

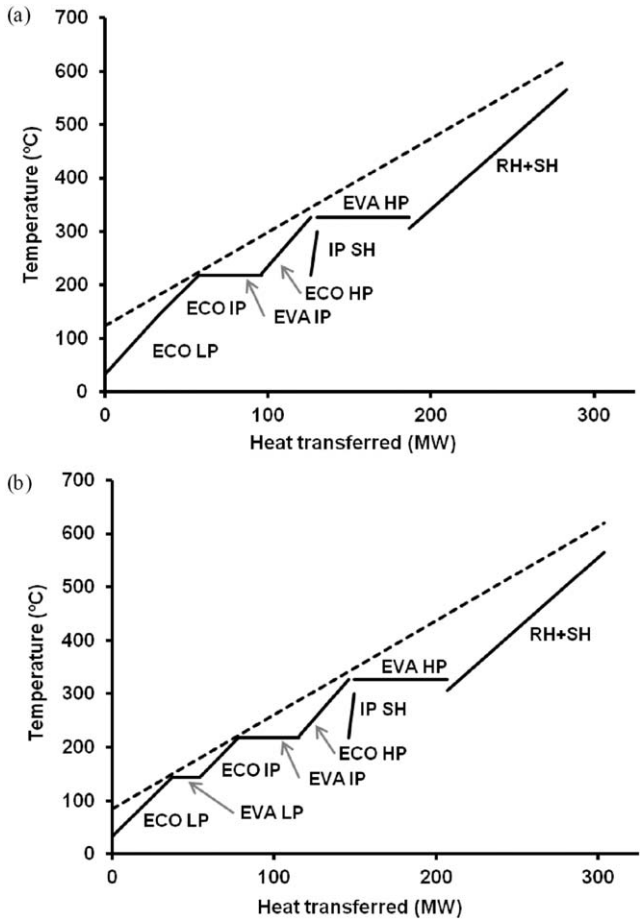

Figure 2. Composite curves for (a) double-pressure reheat and (b) triple-pressure reheat HRSG, with 45 kg/s of HP-saturated steam produced external to the HRSG.

Dashed lines refer to the exhaust flue gas and solid lines refer to water/steam cycle.

for both configurations (45 kg/s), it has been obtained the composite curves depicted in Figure 2 for the double-pressure reheat (a) and the triple-pressure reheat (b) layouts. As shown in this figure, the minimum temperature difference for both configurations is located at the inlet of the intermediate pressure (IP) EVA. From this pinch point and the hot end of the HRSG, it is recovered in both cases the same amount of heat from the hot exhaust gas (around 225 MW). However, only about 280 MW of the heat available from the flue gas is transferred to the water/steam steam cycle in the double-pressure configuration (Figure 2a) whereas around 305 MW are recovered in the triple-pressure reheat configuration (Figure 2b), which translates into a higher stack temperature for the double-pressure case (125°C vs. 85°C). This more efficient heat transfer in the triple-pressure reheat configuration translates into a higher amount of steam produced (76 kg/s vs. 68 kg/s) and, therefore, a high-efficient combined cycle. From this analysis, the triple-pressure reheat configuration was chosen in this work for the HRSG coupled to the gas turbine.

In the integrated combined cycle power plant, CO_2 compression has been included in the simulation layout, designed according to the information provided by Romano et al.[34] The CO_2 compressor is a five-stage-intercooled compressor, with an intermediate temperature of 30°C and including also intermediate flash units to separate condensates. The stream of CO_2 liquefied has a purity of >99%, which fits CO_2 concentrations limits allowed for its geological storage. The specific consumption of the CO_2 compressor, according to the operating parameters considered in Table 2, resulted to be around 100 (kW h)/t_{CO2} captured, in accordance with the power requirements predicted by Darde et al.[55] when compressing a nearly pure CO_2 stream as in this case.

Figure 3 summarizes the integration explained earlier between the combined cycle and the Ca–Cu looping system. As shown in this figure, the links between the combined cycle and the Ca–Cu looping process are: rich-H_2 gas to be burnt in the combustion chamber, compressed air from gas turbine compressor sent to Stage B, IP steam derived from the outlet of the HP steam turbine to be used in Stage A, LP steam bled from the last stages of the steam turbine to be fed into Stage C′, and the HP-saturated steam produced externally to the HRSG of the combined cycle to be fed into the SH of the HRSG. For the sake of simplicity, the heat-exchange network between the Ca–Cu looping gas streams, the fan required in Stage B, as well as the CO_2 CPU have not been depicted in Figure 3.

Heat-exchange network design

Due to the large amount of heat available from cooling process gas streams leaving the different stages in the Ca–Cu looping system, a heat-exchange network has been designed with the aim of accommodating the inputs up to the specifications of each stage while producing as much HP-saturated steam as possible to be introduced in the SH of the steam cycle. As detailed in the "H_2 production island" section, there are six gas streams that provide valuable heat suitable to be integrated into the process. However, the exhaust gas from the gas turbine (Stream 11 in Figure 1) has not been included in the heat-exchange network designed, because it is sent to the HRSG. Figure 4 shows a schematic layout of the process integration proposed, including the same notation as in Figure 1 for better understanding. CH_4 needed into Stage A enters into the system at 20°C and at a pressure slightly higher than that required in Stage A. It is heated up to around 310°C before being mixed with steam at around 2200 kPa bled from the outlet of the HP steam turbine. As seen in Figure 4, this heating is accomplished thanks to the heat recovered from the exhaust gas of the expander (Unit G in Figure 1), which is at a temperature in the range of 340–365°C depending on the temperature of the gas fed into this expansion stage ($T_{max,B}$). This mixture of CH_4 and steam is further heated up to 650°C in subsequent stages using heat from rich-H_2 gas from Stage A at 650°C and from rich-CO_2 gas from Stage C at 850–870°C ($T_{max,C}$). An equivalent heating route has been assumed for the CH_4 fed into Stage C′, introduced into the process at around atmospheric pressure and 20°C, and heated up to around 210°C before being mixed with steam bled from the LP steam turbine. As depicted in Figure 4, this mixture is heated up to 650°C to be fed into Stage C′ thanks to the heat recovered from compressed air at around 420°C and rich-CO_2 gas.

According to Figure 4, external HP steam is generated thanks to the heat recovered from: (1) the rich-H_2 gas stream after gas heating, which is cooled down to 300°C to be fed into the combustion chamber of the gas turbine; (2) the O_2-depleted gas obtained from Stage B′ at 675–695°C

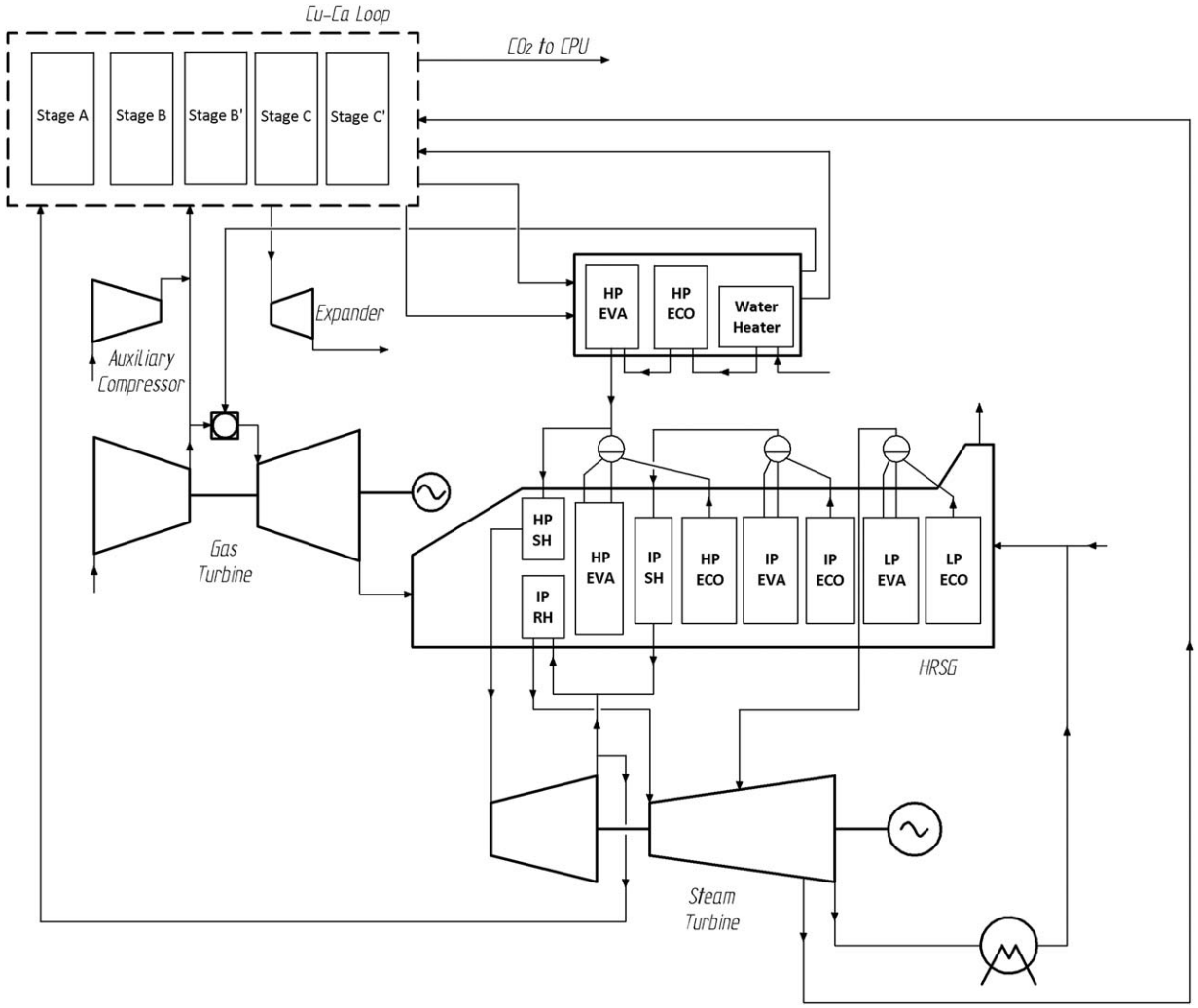

Figure 3. Schematic layout of the integrated combined cycle with the Ca–Cu looping process.

(depending on the S/C ratio in Stage A) that is required to be at 150°C to be fed again into Stage B; (3) the rich-CO_2 gas stream from Stage C after gas heating that should be cooled down to be fed into the CPU for its storage; and (4) compressed air from the gas turbine and the booster compressors after gas heating that are required to be at 150°C to be fed into Stage B. It has been assumed that feedwater for HP steam generation comes into the system as saturated liquid at 4.8 kPa, resulting from condensing steam exiting last expansion stage in the gas turbine. This saturated liquid is compressed up to around 12,500 kPa and is fed into heating stages, economizer (ECO) and evaporator (EVA) units. As a result of this integration, nearly half of the HP steam introduced into the HP steam turbine of the steam cycle is produced external to the HRSG. Temperature differences considered in the heat exchangers depend on the type of heat exchange as compiled in Table 2.

It was checked that in most of the analyzed cases there was low-temperature heat still available in the rich-CO_2 stream after its use in the heat-exchange network before being sent to the CPU. It was analyzed the possibility of using this waste heat to produce LP steam to be fed into the steam turbine, but it was demonstrated that negligible improvements in the net efficiency were obtained and, therefore, this option was rejected.

Simulation Results

Plant performance

To make a comparison between the reference NGCC without CO_2 capture and the combined cycle integrated with the Ca–Cu looping system, the following operating conditions have been chosen as a base case: a S/C molar ratio of 5 in Stage A, a maximum temperature of 830°C in Stage B and 870°C as calcination temperature in Stage C, which lead to high H_2 yield in Stage A and high overall CO_2 capture efficiency. These conditions are similar to those proposed by Fernández et al.[48] but maintaining the three pressures mentioned earlier (2200, 1830, and 101.3 kPa in Stages A–C). Under these process conditions and for the same airflow rate entering the gas turbine compressor in both cases, results (reported on Table 3) show a net efficiency of 48.9% (based on the low heating value, LHV, of CH_4) for the combined cycle integrated with the Ca–Cu looping process, with an efficiency penalty of 9.9% points with respect to the NGCC reference case and an 88.5% of overall CO_2 capture efficiency.

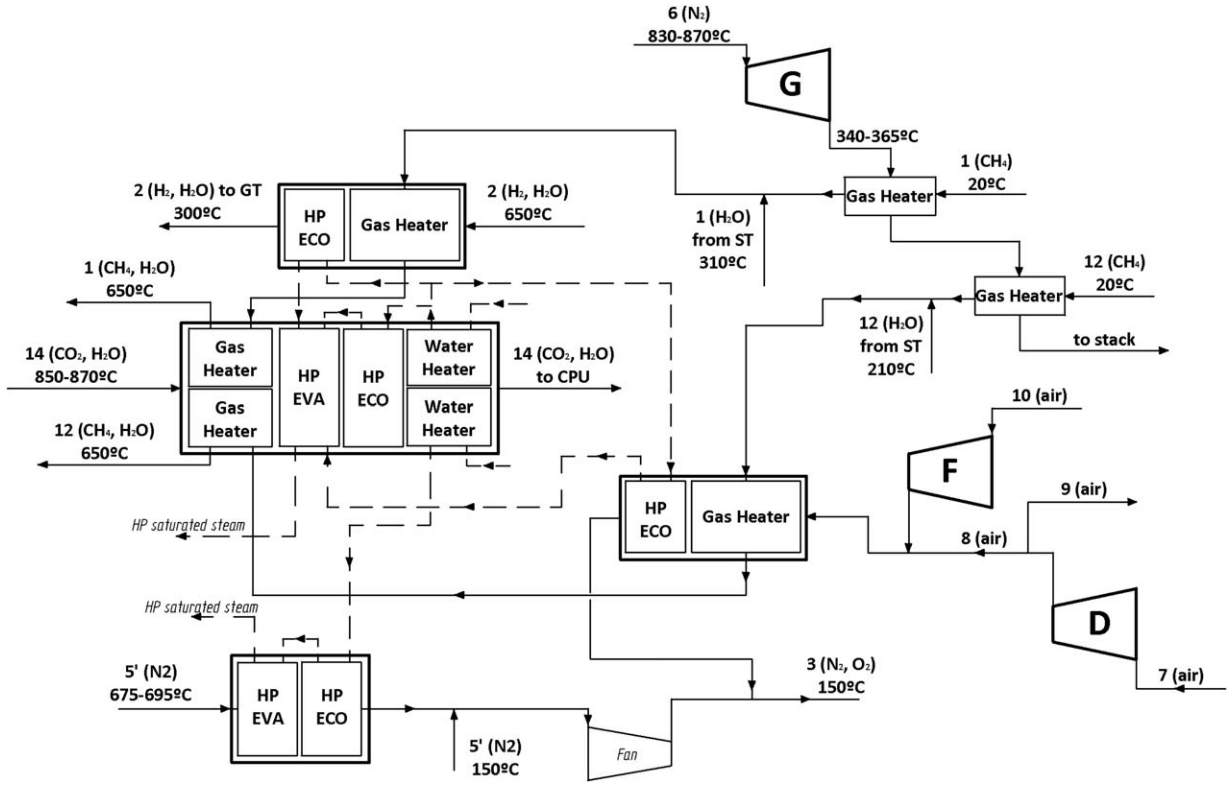

Figure 4. Detailed layout of the heat-exchange network designed between the Ca–Cu looping process streams.

Dashed lines refer to water/steam streams of the steam cycle and continuous lines refer to process streams of the Ca–Cu looping process (GT: gas turbine and ST: steam turbine).

Higher gas turbine power output (64.3 MW) is obtained in the integrated combined cycle with the Ca–Cu looping process with respect to the reference NGCC, despite the lower temperature at the turbine inlet. The main reasons for this higher output are, on the one hand, the higher amount of flue gas expanded in the gas turbine of the Ca–Cu case (due to an increase in the fuel flow rate, from 11.9 kg/s of NG in the NGCC to 41.5 kg/s of rich-H_2 in the Ca–Cu case) and, on the other hand, the higher steam content of this flue gas, which leads to a higher enthalpy drop along the expansion in the gas turbine compared with the rich-N_2 exhaust gas in the reference NGCC. With respect to the steam cycle, there is not a great difference between the power output produced in both cases despite the fact that the steam derived to the Ca–Cu looping process bled from HP turbine outlet yields between 40 and 60% of the steam expanded in the HP turbine, and the LP steam bled from LP steam turbine represents between 11 and 18% of the steam expanded in the LP turbine. This fact is explained, because the power loss derived from these steam extractions is compensated by both: a larger mass flow rate of steam produced in the HRSG because of a higher exhaust gas flow rate, and the HP-saturated steam generated external to the HRSG by cooling gas process streams. Among the additional power requirements in the Ca–Cu looping process, CO_2 compressor represents the highest power loss (14.1 MW), followed by the booster air compressor (10.9 MW) and the fan (3.1 MW). However, there is an important difference in the power distribution between the two plants compared, because there is extra electricity produced in the expansion of the gas from Stage B (34.4 MW), which compensates greatly the additional power requirements associated with the Ca–Cu looping process. Moreover, as a result of the conversion efficiency of CH_4 to H_2 in the SER process, but mainly due to the fact that the CH_4 fed into Stage C′ is not going to generate valuable gas for power generation, thermal input in the Ca–Cu looping system is greatly higher than in the NGCC case (765.3 MW_{th} vs. 524.3 MW_{th}), contributing also to penalize net efficiency of the process.

Table 3. Results of the Reference NGCC and the Base Case Considered for the Integrated Combined Cycle with the Ca–Cu Looping Process

	Reference NGCC without CO_2 capture	Integrated combined cycle with the Ca–Cu looping system
Electric power (MW)		
Gas turbine	197.1	261.4
Gas turbine auxiliaries	−0.7	−0.9
Steam turbine	113.3	109.5
Steam cycle pumps	−1.4	−1.2
N_2 expander	–	34.4
Booster compressor	–	−10.9
Fan	–	−3.1
Auxiliary pumps		−0.8
CO_2 compressor	–	−14.1
Net power	308.3	374.3
Thermal input (MW_{th}, based on LHV)	524.3	765.3
Net efficiency (%)	58.80	48.9
CO_2 capture ratio (%)	–	89
Specific emissions (g_{CO2}/[kW h])	351.3	40.5

Table 4. Operating Conditions and Results Obtained for the Different Case Studies Analyzed

	Case A1	Case A2	Case A3	Case A4	Case B1	Case B2	Case B3	Case B4	Case B5	Case B6
S/C in Stage A	5	5	5	5	3	3	3	3	3	3
T_{max} in Stage B (°C)	830	830	850	850	830	830	850	850	870	870
T_{max} in Stage C (°C)	870	850	870	850	870	850	870	850	870	850
$P_{GT,net}$ (MW)	260.5	260.4	260.4	260.4	241.9	241.9	241.9	241.9	241.9	241.9
$P_{ST,net}$ (MW)	108.3	107.4	106.9	106.7	118.3	117.8	117.7	117.2	116.8	116.2
$P_{expander}$ (MW)	34.4	33.4	34.9	33.8	30.6	29.5	30.9	29.9	31.3	30.4
$P_{booster}$ (MW)	10.9	9.8	10.5	9.4	4.8	3.7	4.4	3.3	3.8	2.9
P_{fan} (MW)	3.1	3.0	3.0	2.9	2.8	2.8	2.8	2.7	2.7	2.6
P_{aux} (MW)	0.8	0.8	0.8	0.8	0.7	0.7	0.7	0.7	0.7	0.7
P_{CPU} (MW)	14.1	13.7	13.6	13.6	12.4	12.3	12.3	12.3	12.1	12.1
P_{net} (MW)	374.3	373.9	374.3	374.2	370.1	369.7	370.3	370.0	370.7	370.2
H_{in} (LHV) (MW)	765.3	737.7	762.1	737.7	751.4	725.9	751.4	725.9	751.4	725.9
$\eta_{net,\ plant}$ (%)	48.9	50.7	49.1	50.7	49.2	50.9	49.3	51.0	49.4	51.0
Penalties (% points)	9.9	8.1	9.7	8.1	9.6	7.9	9.5	7.8	9.5	7.8
CCR (%)	89.0	90.1	86.6	89.2	80.2	82.2	79.3	81.9	77.9	80.9
gCO_2 emitted/(kW h)	40.5	40.1	46.0	43.6	78.5	78.1	83.3	82.8	88.8	88.2

P: power output, η: efficiency.

Sensitivity analysis

A sensitivity analysis has been carried out to determine the influence of the operating conditions of the Ca–Cu looping process in the overall plant performance and to find out those operating parameters that result in the lowest efficiency penalties. For a given mass flow rate of CH_4 of 10 kg/s fed into Stage A, and maintaining the temperature of the inlet streams of Stages A, B, and C′ at 650, 150, and 650°C, respectively, the following parameters have been modified: (1) the S/C molar ratio in Stage A, to analyze the possible effect of diverting part of the IP steam at 2200 kPa from the steam turbine to the Ca–Cu looping system, (2) T_{max} allowed in Stage B that determines mainly the CO_2 released in Stage B that will be emitted to the atmosphere with the exhaust gas turbine, and (3) the calcination temperature in Stage C (accomplished by modifying the S/C molar ratio in Stage C′) related to the recoverable heat in the heat-exchange network as well as with the amount of Cu needed in the system. As a result of modifying these operating parameters, 10 different case studies have been obtained as reported in Table 4.

Effect of S/C Molar Ratio in Stage A. The molar S/C ratio in the gas fed into SER stage has been modified between 3 and 5, which are common values considered in the literature for the SER.[35] As shown from the results in Table 4, gas turbine power output is higher for cases with a higher S/C ratio in Stage A, although flue gas molar flow expanded in the gas turbine in all the simulation cases is similar. Main differences between cases labeled as "A" in Table 4 (with a S/C ratio of 5 in Stage A) and those labeled as "B" (S/C of 3 in Stage A), come from the rich-H_2 gas burnt in the combustion chamber of the gas turbine, which has a higher flow rate and a higher H_2 content for A cases with a S/C ratio of 5 in Stage A. On the one hand, higher volume flow rate of fuel fed into the gas turbine leads to a lower excess of air in the combustion chamber to accomplish the combustor outlet temperature of 1433°C established, which translates into a lower compressor consumption, whereas, on the other hand, higher H_2 and steam content in the fuel leads to a higher steam molar fraction in the flue gas expanded (25% vol. vs. 18% vol.), which involves a higher enthalpy drop along the expansion in the gas turbine, and higher specific power produced in the expansion. As a result of both effects, higher gas turbine output results in those cases with a higher S/C molar ratio in Stage A (260.4 MW vs. 241.9 MW). However, as higher S/C ratio in Stage A implies a higher amount of steam at 2200 kPa bled from the steam turbine (a mass flow of 10 kg/s of CH_4 into Stage A is maintained constant in all the simulation cases), lower amount of steam is expanded in the steam turbine in A cases of Table 4 that reduces its power output.

From a power consumption point of view, main power requirements from CO_2 compressor (P_{CPU} in Table 4), fan (P_{fan}), and booster compressor ($P_{booster}$) are higher for those A cases with higher S/C in Stage A, which compensates the higher gas turbine power output, and translates into a net power output (P_{net}) similar to that obtained for B cases operating with a lower S/C ratio in Stage A. Increasing the S/C ratio in Stage A CH_4 conversion in the SER stage is favored and $CaCO_3$ formed increases, which translates into a higher amount of CuO required in the process to accomplish the energy balance required in Stage C. As a consequence, higher amount of O_2 is required into Stage B and higher mass flow rate of CO_2 is produced in Stage C of the Ca–Cu looping process, which lead to higher booster and CO_2 compressor consumptions, respectively. Differences mentioned between A and B cases with respect to gas and steam turbine power output and to power requirements, make the net plant power output (P_{net}) be almost similar in every case analyzed, and make the heat input be the decisive parameter on the net efficiency.

Thermal input is determined by the amount of CH_4 fed into Stage C′, as a mass flow of CH_4 of 10 kg/s into Stage A has been maintained constant in every simulated case as pointed out previously. CH_4 input into Stage C′ increases when increasing the amount of CuO required in the process to fulfill energy balance in Stage C, because higher amount of the CO/H_2 mixture is needed for CuO reduction. Moreover, thermal input depends on $T_{max,B}$ and $T_{max,C}$, but this effect is described in the next sections. Consequently, as S/C ratio in Stage A increases, and a higher amount of $CaCO_3$ is formed into Stage A, higher thermal input is required into the process. As a result of this increase, generally slightly lower net efficiencies result from A cases with respect to B ones, when comparing cases with the other two parameters ($T_{max,B}$ and $T_{max,C}$) constant, and efficiency penalties as low as 7.8% points can be achieved under operating conditions with a S/C ratio of 3 in Stage A.

Larger differences are observed from a CO_2 emission or CO_2 capture efficiency point of view, as cases with the highest S/C ratio in Stage A show the best CO_2 capture rates, as specific CO_2 emissions decrease when $CaCO_3$ formation is favored in Stage A. CO_2 capture efficiencies, or carbon capture ratio (CCR) in Table 4, close to 90% come from the cases with S/C molar ratio of 5, whereas values as low as 78% of capture efficiency have resulted from cases with a ratio of 3. According to the results in Table 4, the lowest values for the CO_2 emissions come from those cases operating at a $T_{max,B}$ as low as 830°C in Stage B, resulting around 40 and in 78 g CO_2 emitted/(kW h) for S/C of 5 (Cases A1 and A2) and 3 (Cases B1 and B2), respectively.

Effect of Calcination Temperature ($T_{max,C}$). Calcination temperature in Stage C (which is the maximum temperature in Stage C, $T_{max,C}$) should be high enough to favor calcination kinetics under the operating conditions of Stage C. When increasing $T_{max,C}$ from 850 to 870°C, steam excess in Stage C can be reduced from 2 to 1.5 according to calcination kinetics, but higher amount of Cu-material is needed as the energy required in Stage C to achieve $T_{max,C}$ increases. From the results obtained (Table 4), it can be appreciated that for a given S/C molar ratio in Stage A and $T_{max,B}$, lower $T_{max,C}$ translate into lower efficiency penalties, due mainly to the fact that lower thermal input is then required in Stage C′. To a lesser extent, the reduction in $T_{max,C}$ will lead also to reduced air fan power consumption. So, from a calcination temperature point of view, the lowest feasible temperature chosen in Stage C leads to low efficiency penalties as thermal input in Stage C is reduced. $T_{max,C}$ should not be further decreased below 850°C as then calcination reaction would not take place (equilibrium CO_2 partial pressure at 850°C is 48.6 kPa and CO_2 partial pressures ranged from 40.5 to 42.6 kPa in the cases studied).

Effect of Oxidation Temperature ($T_{max,B}$). As part of the gas leaving oxidation stage at $T_{max,B}$ is used to drive an external expander to produce extra power, it is important that Stage B in the Ca–Cu looping process operates at its maximum allowable temperature $T_{max,B}$ to enhance the subsequent expansion efficiency. However, this temperature is related to the CO_2 emissions in the Ca–Cu looping system, because part of the CO_2 emitted in the process comes from the O_2-depleted air after expansion, which is sent to the stack. Therefore, it is important to minimize $CaCO_3$ calcination in this stage to avoid increasing the CO_2 emitted in the process. According to the results in Table 4, the lowest values for the CO_2 emissions come from those cases operating at a $T_{max,B}$ as low as 830°C in Stage B, resulting in around 40 and 78 g CO_2 emitted/(kW h) for S/C of 5 (Cases A1 and A2) and 3 (Cases B1 and B2), respectively. However, nonremarkable differences in the net efficiency can be attributed to changes in $T_{max,B}$, because the O_2-depleted gas from Stage B sent to the expander represents around 10% of the total gas expanded in the gas turbine, and, therefore, power produced in the expansion unit is around 8% of the total power produced in the system (sum of $P_{GT,net}$, $P_{ST,net}$, and $P_{expansor}$ in Table 4). As a consequence, low $T_{max,B}$ is preferable in this system, as CO_2 emissions are then minimized and net efficiency in the process is not dramatically affected. Under these conditions of minimum $T_{max,B}$, slightly higher amounts of Cu-supported material are required to heat the solid bed up to the calcination temperature in Stage C, which would increase the operating costs of the process.

To complete the analysis and determine an optimum set of operating conditions in the simulation model proposed, it has been studied the contribution of each individual penalty to the whole penalization to the net efficiency of the reference NGCC plant. According to the assessment of the net penalty carried out in this work, four main sources of penalization arise from the analysis. Three of them have been computed directly in the evaluation of the net plant efficiency: CO_2 CPU, booster compressor and fan in Stage B and plant auxiliaries, whereas there is a fourth one, specific and inherent to this Ca–Cu looping process. On the one hand, there is an additional fuel consumption in Stage C′ to produce the syngas for CuO reduction, which is not going to produce power but increases the thermal input into the process. On the other hand, there is a portion of air derived from the compressor outlet to the Ca–Cu looping process that is delivered O_2 depleted with a lower flow rate, and sent to an expander with a lower efficiency than the compressor gas turbine. In this way, a higher flow rate is compressed with respect to that expanded, contributing to the penalization. This group of penalties derived from coupling the Ca–Cu looping process with a combined cycle have been brought together and titled as Inherent in Figure 5, where the contribution of each penalization mentioned is represented.

According to Figure 5, CPU penalization remains almost constant between 17 and 23% of the whole penalization in every case analyzed, because the CO_2 capture rate moves between 78 and 90% in the different scenarios analyzed. Wider differences result from booster compressor and fan between cases with high S/C molar ratio (A cases in Figure 5) to those cases with low S/C ratio (B cases). This is due to the fact that higher amounts of Cu-based material are needed in A cases, because of the effect of high S/C explained earlier, and then higher amounts of O_2 (and subsequently of air) are required to be fed into Stage B. It could be also appreciated that modifying the $T_{max,B}$ and $T_{max,C}$, the contribution of booster compressor and fan consumption to the whole penalty of the process remains almost constant between 18 and 21% for A cases and between 9 and 11% for B cases. The highest differences in the contribution of each penalty source come from those inherent to the Ca–Cu looping process, especially when varying $T_{max,C}$. This is mainly due to the fact that there are great differences in the thermal input when varying from 850 to 870°C in $T_{max,C}$. As mentioned, lower steam excess is required into Stage C′ for $T_{max,C}$ of 870°C, because the CO_2 equilibrium partial pressure is so high with respect to the CO_2 partial pressure that there would be no problems for calcination, but higher amounts of CH_4 are required then to achieve this higher $T_{max,C}$, and, therefore, higher penalization. Consequently, $T_{max,C}$ of 850°C is preferred from an efficiency point of view, due to their lower penalization to the net plant efficiency. There are further differences in the inherent penalty when modifying the S/C between 3 and 5, as it is observed lower contribution for Cases A than for B. This is due to the positive effect that high S/C ratios in Stage A have into the net power output derived from the gas turbine, as explained before. Related to this fact, operating conditions with S/C of 5 become the optimum from a penalization point of view, because, under these conditions, inherent penalties to the process are the minimum whereas the other penalties are susceptible of being reduced with technological improvements in the CO_2 or in the air compressors. According to this analysis, the

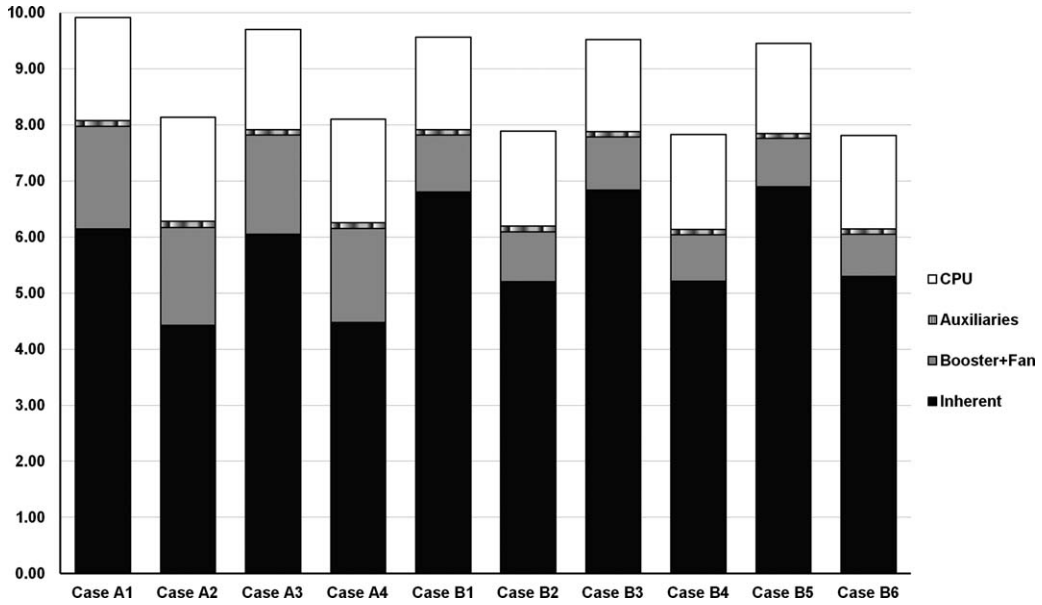

Figure 5. Contribution of the different penalty sources considered in the different cases studied (nomenclature used for the different cases referred to that used in Table 4).

optimum operating conditions chosen, which maximize the net efficiency of the process up to a value of 50.7%, leading to 8.1% points of penalty, and allow accomplish an overall carbon capture efficiency of 90% in the process, are $T_{max,B}$ of 830°C, $T_{max,C}$ of 850°C, and a S/C molar ratio of 5 in Stage A.

Results obtained for the integrated combined cycle with the Ca–Cu looping system under these optimum conditions have been compared with other competing technologies proposed in the literature to be integrated in a NGCC, based on burning a decarbonized fuel into the gas turbine. Among these technologies, it has been considered those commercial based on NG POX, SMR, and ATR, and those emerging technologies based on using CO_2-sorbent acceptors, like SEWGS or SER. The main results obtained in each case reported in the literature are shown in Table 5, together with the results obtained in this work for the optimum operating conditions chosen.

From the results compiled in Table 5, it is observed a wide range of efficiency penalties reported for the ATR-based power plants (from 8 to 14% points), which indicates the strong dependence with the operating assumptions made with temperature or pressure, or the CO_2 removal unit heat duty considered. SMR is in the upper limit of the efficiency penalty due to its high energy requirements in the reforming stage and the low temperature of the gas streams to be integrated, with modest carbon capture rates of around 85%. Regardless of SMR, the efficiency assessed in this work for the integration of the Ca–Cu looping process into a NGCC (50.7%, 8.1% points of penalty) is similar to those values reported in literature for the SER process (50.2%, 8.4% points of penalty)[40] and for the SEWGS (50.0%, 8.3% points of penalty).[43] It is reasonable that similar efficiencies to those reported for the SER concept are obtained, because both concepts are similar. Higher turbine output is obtained for the SER case, as there is no air derived from the air compressor to the SER process like in the Ca–Cu looping process, and due to the lower amount of steam bled from the steam turbine to the process (S/C ratio of 4.5 for reforming in SER has been chosen, but higher S/C is required in the Ca–Cu case due to the steam fed into Stage C′ to perform further reforming). However, similar efficiency results in both cases, because ASU power consumption in the SER layout contributes to increase penalty to the reference NGCC. Compared with the results reported for the SEWGS process, it can be observed that, making the correspondent changes to be in the same order of magnitude, similar gas turbine sizes but higher steam turbine power output are reported for the SEWGS case with respect to the results in this work. Air extraction is made for both cases from the gas turbine compressor to the H_2 production island, but a highly efficient gas heater reformer is used in the SEWGS case, operating with a very low steam excess (low steam bled from steam turbine). However, slightly higher efficiency is obtained in the Ca–Cu looping scheme, as the O_2-depleted air extracted from the gas turbine compressor is used to drive an external expander, producing additional power.

To summarize, efficiency penalty obtained in this work for the integration of the Ca–Cu looping process into a NGCC is among the lowest values reported in the literature for similar technologies, whereas the CO_2 capture efficiency can be as high as 90%. Process simplification with respect to the other competing technologies, derived mainly because of the thermally neutral character of the reactions involved, allows for fewer fixed-bed reactors (of larger diameter) using similar pressure and temperature swing modes of operation as in other existing processes, but without the need of heat supply surfaces. Moreover, from an operational point of view, the Ca–Cu looping system shows a simplified layout with respect to ATR and POX technologies that required at least five different stages (prereformer for ATR, ATR/POX reactor, HT, and LT WGS reactors, and the absorber-stripper amine absorption plant), and it also avoids the operating problems derived from the ATR/POX stringent conditions of temperature and pressure. Concerning the integration of the SEWGS process with a combined cycle, it must be pointed out that the capital intensive steam reforming reaction stage is still required to produce a suitable H_2/CO gas stream. In addition, high carbon capture rates force to include a high temperature shift reactor previous to the SEWGS stage to

Table 5. Comparison Between the Results Obtained in This Work and Those from Literature for Other H_2-Production Technologies Integrated into a NGCC

		ATR			POX	SMR	SEWGS		SER
Technology	Cu–Ca loop	Kvamsdal et al.[30]	Nord et al.[33]	Romano et al.[34]	Lozza and Chiesa[32]	Lozza and Chiesa[31]	Manzolini et al.[43]		Romano et al.[40]
Reforming stage									
S/C molar ratio	5	2	1.5	1.5	0.95	2.9	1.1		4.5
Temperature (°C)	650	900	950	1050	980	700	950		700
Oxidant used	–	Air	Air	Air	Air	–	Air		–
Prereformer	Absent	Adiabatic	Adiabatic	Adiabatic	Absent	Absent	Absent		Absent
CO_2 removal unit									
Absorption solvent	Inherent	DEA	MDEA	MDEA	DEA	DEA	Inherent		Inherent
Capture heat duty		–	1.5 MJ_{th}/kg CO_2	0.99 MJ_{th}/kg CO_2	1.78 MJ_{th}/kg CO_2	2.29 MJ_{th}/kg CO_2			
Overall carbon capture (%)	90.10	83	90.20	91.60	85.20	84.60	95.10		88.00
Net efficiency (%)	50.70	47.40	41.90	50.65	48.50	46.10	50.00		50.20
Efficiency penalty (% points)	8.1	9.8	14.0	7.9	7.6	10.0	8.3		8.4
Specific emissions (g_{CO2}/[kW h])	40.1	60.4	33.2	34.2	40.9	43.4	17.1		49.2

favor high CO_2 yields, and, therefore, process simplification is affected. These results validate the Ca–Cu looping process as a technology suitable to be integrated with a combined cycle to produce power.

Conclusions

This article proposes the integration of a novel process for H_2 production based on a double chemical Ca–Cu loop in a NGCC. The inclusion of the Cu-chemical loop in this process leads to an efficient heat transfer between the calcination of $CaCO_3$ and the CuO reduction and contributes to enhance the efficiency of the process. A possible integration between this novel chemical process and a NGCC has been detailed and used to carry out an analysis of the influence of the operating conditions in the overall plant performance. A plant efficiency decay between 7.8 and 9.9% points results from the operating conditions analyzed, when compared to a NGCC of similar technology level. Evaluating this loss, it is noticed that the contribution of the inherent characteristics of the Ca–Cu looping process account for the largest penalty to the reference NGCC (between 4.4 and 6.9% points). Optimizing the operating conditions in the Ca–Cu looping process to achieve a high efficiency value with low CO_2 emissions, it has been concluded that best operating conditions for this process are: $T_{max,B}$ of 830°C, $T_{max,C}$ of 850°C, and a S/C molar ratio of 5 in Stage A. Under these conditions, an efficiency as high as 50.7% can be obtained, 8.1% points less than the efficiency of the reference NGCC considered, with CO_2 emissions as low as 40.1 gCO_2/(kW h). Compared with other precombustion routes applied to NGCC, the Ca–Cu looping process emerges as a technology suitable to be integrated into a combined cycle, with efficiency penalties similar to the lowest reported in the literature for the other precombustion routes and a CO_2 capture efficiency as high as 90%, with the great advantage of relying on a simplified layout and compact design inherent to the Ca–Cu looping system technology.

Acknowledgments

This work is supported by the R+D Spanish National Program from the former Spanish Ministry of Science and Innovation and PlanE under project ENE2009–11353 and from CSIC 201280E017. Financial support for I. Martínez during her PhD studies is provided by the FPU programme of the Spanish Ministry of Education (reference AP2009–3575).

Notation

Acronyms

ASU = air separation unit
ATR = autothermal reforming
CPU = compression and purification unit
DEA = diethanolamine
EBTF = European Benchmarking Task Force
ECO = economizer
EVA = evaporator
HP = high pressure
HRSG = heat recovery steam generator
IP = intermediate pressure
LHV = low heating value
LP = low pressure
MDEA = *N*-methyldiethanolamine
MEA = monoethanolamine

NG = natural gas
NGCC = natural gas combined cycle
POX = partial oxidation
RH = reheater
SER = sorption-enhanced reforming
SEWGS = sorption-enhanced water–gas shift
SH = superheater
SMR = steam methane reforming
TIT = turbine inlet temperature
UMR = unmixed reforming
VGV = variable guide vanes

Literature Cited

1. IEA. World Energy Outlook 2011. IEA, 2011; Available at http://www.worldenergyoutlook.org/. Paris: OECD Publishing. Last accessed December 3, 2012.
2. Sims REH, Schock RN, Adegbululgbe A, Fenhann J, Konstantinaviciute I, Moomaw W, Nimir HB, Schlamadinger B, Torres-Martínez J, Turner C, Uchiyama Y, Vuori SJV, Wamukonya N, Zhang X. In Metz B, Davidson OR, Bosch PR, Dave R, Meyer LA, editors. Energy Supply. Climate Change 2007: Mitigation of Climate Change. Cambridge and New York: Cambridge University Press, 2007.
3. Kvamsdal HM, Maurstad K, Jordal K, Bolland O. Benchmarking of gas-turbine cycles with CO_2 capture. In: Rubin ES, Keith DW, Gilboy CF, editors. Proceedings of 7th International Conference on Greenhouse Gas Control Technologies, I: Peer Reviewed Papers and Overviews. Oxford, UK: Elsevier Science, 2005:233–242.
4. Lozza G, Chiesa P, Romano M, Valenti G. CO_2 capture from natural gas combined cycles. In: 1st International Conference on Sustainable Fossil Fuels for Future Energy, Rome, 2009.
5. Bolland O, Mathieu P. Comparison of two CO_2 removal options in combined cycle power plants. *Energy Convers Manage*. 1998;39(16–18):1653–1663.
6. Bolland O, Undrum H. A novel methodology for comparing CO_2 capture options for natural gas-fired combined cycle plants. *Adv Environ Res*. 2003;7(4):901–911.
7. Chiesa P, Consonni S. Natural gas fired combined cycles with low CO_2 emissions. *J Eng Gas Turbines Power*. 2000;122(3):429–436.
8. Karimi M, Hillestad M, Svendsen HF. Natural gas combined cycle power plant integrated to capture plant. *Energy Fuels*. 2012;26(3):1805–1813.
9. Kanniche M, Gros-Bonnivard R, Jaud P, Valle-Marcos J, Amann J-M, Bouallou C. Pre-combustion, post-combustion and oxy-combustion in thermal power plant for CO_2 capture. *Appl Therm Eng*. 2010;30(1):53–62.
10. Bolland O, Sæther S. New concepts for natural gas fired power plants which simplify the recovery of carbon dioxide. *Energy Convers Manage*. 1992;33(5–8):467–475.
11. Kvamsdal HM, Jordal K, Bolland O. A quantitative comparison of gas turbine cycles with capture. *Energy*. 2007;32(1):10–24.
12. Ertesvåg IS, Kvamsdal HM, Bolland O. Exergy analysis of a gas-turbine combined-cycle power plant with precombustion CO_2 capture. *Energy*. 2005;30(1):5–39.
13. Metz B, Davidson O, de Coninck H, Loos M, Meyer L. IPCC Special Report on Carbon Dioxide Capture and Storage. Prepared by Working Group III of the Intergovernmental Panel on Climate Change. Cambridge, United Kingdom and New York, NY, USA: Cambridge University Press, 2005.
14. Lisbona P, Romeo LM. Enhanced coal gasification heated by unmixed combustion integrated with an hybrid system of SOFC/GT. *Int J Hydrogen Energy*. 2008;33(20):5755–5764.
15. Chiesa P, Lozza G. CO_2 emission abatement in IGCC power plants by semiclosed cycles: part A—with oxygen-blown combustion. *J Eng Gas Turbines Power*. 1999;121(4):635–641.
16. Chan SH, Ho HK, Tian Y. Modelling of simple hybrid solid oxide fuel cell and gas turbine power plant. *J Power Sources*. 2002;109(1):111–120.
17. Inui Y, Matsumae T, Koga H, Nishiura K. High performance SOFC/GT combined power generation system with CO_2 recovery by oxygen combustion method. *Energy Convers Manage*. 2005;46(11–12):1837–1847.
18. Consonni S, Lozza G, Pelliccia G, Rossini S, Saviano F. Chemical-looping combustion for combined cycles with CO_2 capture. *J Eng Gas Turbines Power*. 2006;128(3):525–534.
19. Naqvi R, Wolf J, Bolland O. Part-load analysis of a chemical looping combustion (CLC) combined cycle with CO_2 capture. *Energy*. 2007;32(4):360–370.
20. Franco F, Anantharaman R, Bolland O, Booth N, van Dorst E, Ekstrom C, Sanchez-Fernades E, Macchi A, Manzolini G, Nikolic D, Pfeffer A, Prins M, Rezvani S, Robinson L. European best practice guidelines for assesment of CO_2 capture technologies, 2011.
21. Peeters ANM, Faaij APC, Turkenburg WC. Techno-economic analysis of natural gas combined cycles with post-combustion CO_2 absorption, including a detailed evaluation of the development potential. *Int J Greenhouse Gas Control*. 2007;1(4):396–417.
22. Manzolini G, Macchi E, Binotti M, Gazzani M. Integration of SEWGS for carbon capture in natural gas combined cycle. Part B: reference case comparison. *Int J Greenhouse Gas Control*. 2011;5(2):214–225.
23. Fluor Daniel I. Improvement in power generation with post-combustion capture of CO_2. IEA Report Number PH4/33, 2004.
24. Aroonwilas A, Veawab A. Integration of CO_2 capture unit using single- and blended-amines into supercritical coal-fired power plants: implications for emission and energy management. *Int J Greenhouse Gas Control*. 2007;1(2):143–150.
25. Rao AB, Rubin ES. A technical, economic, and environmental assessment of amine-based CO_2 capture technology for power plant greenhouse gas control. *Environ Sci Technol*. 2002;36(20):4467–4475.
26. Nguyen T, Hilliard M, Rochelle GT. Amine volatility in CO_2 capture. *Int J Greenhouse Gas Control*. 2010;4(5):707–715.
27. Thitakamol B, Veawab A, Aroonwilas A. Environmental impacts of absorption-based CO_2 capture unit for post-combustion treatment of flue gas from coal-fired power plant. *Int J Greenhouse Gas Control*. 2007;1(3):318–342.
28. Chiesa P, Lozza G, Mazzocchi L. Using hydrogen as gas turbine fuel. *J Eng Gas Turbines Power*. 2005;127(1):73–80.
29. Eide LI, Bailey DW. Precombustion decarbonisation processes. *Oil Gas Sci Technol—Rev IFP*. 2005;60(3):475–484.
30. Kvamsdal HM, Andersen T, Bolland O. Natural gas fired power plants with CO2-capture-process integration for high fuel-to-electricity conversion efficiency. In: Sauro P, editor. Comput Chem Eng, Vol. 8. Elsevier, 2000:331–336.
31. Lozza G, Chiesa P. Natural gas decarbonization to reduce CO_2 emission from combined cycles—part II: steam-methane reforming. *J Eng Gas Turbines Power*. 2002;124(1):89–95.
32. Lozza G, Chiesa P. Natural gas decarbonization to reduce CO_2 emission from combined cycles—part I: partial oxidation. *J Eng Gas Turbines Power*. 2002;124(1):82–88.
33. Nord LO, Anantharaman R, Bolland O. Design and off-design analyses of a pre-combustion CO_2 capture process in a natural gas combined cycle power plant. *Int J Greenhouse Gas Control*. 2009;3(4):385–392.
34. Romano MC, Chiesa P, Lozza G. Pre-combustion CO_2 capture from natural gas power plants, with ATR and MDEA processes. *Int J Greenhouse Gas Control*. 2010;4(5):785–797.
35. Harrison DP. Sorption-enhanced hydrogen production: a review. *Ind Eng Chem Res*. 2008;47(17):6486–6501.
36. Williams R. Hydrogen Production, US Patent 1,938,202. 1933.
37. Gorin RL, Retallick WB. Method for the Production of Hydrogen. US Patent 3,108,857. 1963.
38. Solieman AAA, Dijkstra JW, Haije WG, Cobden PD, van den Brink RW. Calcium oxide for CO_2 capture: operational window and efficiency penalty in sorption-enhanced steam methane reforming. *Int J Greenhouse Gas Control*. 2009;3(4):393–400.
39. Reijers HTJ, van Beurden P, Elzinga GD, Kluiters SCA, Dijkstra JW, van den Brink RW. A new route for hydrogen production with simultaneous CO_2 capture. In: 16th World Hydrogen Energy Conference, Lyon, France, 2006.
40. Romano MC, Cassotti EN, Chiesa P, Meyer J, Mastin J. Application of the sorption enhanced-steam reforming process in combined cycle-based power plants. *Energy Procedia*. 2011;4:1125–1132.
41. van Selow ER, Cobden PD, Verbraeken PA, Hufton JR, van den Brink RW. Carbon capture by sorption-enhanced water−gas shift reaction process using hydrotalcite-based material. *Ind Eng Chem Res*. 2009;48(9):4184–4193.
42. Cobden PD, van Beurden P, Reijers HTJ, Elzinga GD, Kluiters SCA, Dijkstra JW, Jansen D, van den Brink RW. Sorption-enhanced hydrogen production for pre-combustion CO_2 capture: thermodynamic analysis and experimental results. *Int J Greenhouse Gas Control*. 2007;1(2):170–179.

43. Manzolini G, Macchi E, Binotti M, Gazzani M. Integration of SEWGS for carbon capture in natural gas combined cycle. Part A: thermodynamic performances. *Int J Greenhouse Gas Control*. 2011;5(2):200–213.
44. Lyon RK. Method and apparatus for unmixed combustion as an alternative to fire. Patent Number 5,509,362. 1996.
45. Kumar RV, Cole JA, Lyon RK. Unmixed reforming: an advanced steam reforming process. In: Proceedings of 218th ACS National Meeting, New Orleans, LA, Vol. 44, no. 4. American Chemical Society, Division of Fuel Chemistry: Washington, 1999:894–898.
46. Lyon RK, Cole JA. Unmixed combustion: an alternative to fire. *Combust Flame*. 2000;121(1–2):249–261.
47. Abanades JC, Murillo R, Fernandez JR, Grasa G, Martínez I. New CO_2 capture process for hydrogen production combining Ca and Cu chemical loops. *Environ Sci Technol*. 2010;44(17):6901–6904.
48. Fernández JR, Abanades JC, Murillo R, Grasa G. Conceptual design of a hydrogen production process from natural gas with CO_2 capture using a Ca–Cu chemical loop. *Int J Greenhouse Gas Control*. 2012;6:126–141.
49. Abanades JC, Murillo R. Method for recovering CO_2 by means of CaO and the exothermic reduction of a solid. PCT/ES2010/0705852009, 2009.
50. Balasubramanian B, Lopez Ortiz A, Kaytakoglu S, Harrison DP. Hydrogen from methane in a single-step process. *Chem Eng Sci*. 1999;54(15–16):3543–3552.
51. Alstrup I, Tavares MT, Bernardo CA, Sorensen O, Rostrup-Nielsen JR. Carbon formation on nickel and nickel–copper alloy catalysts. *Mater Corros*. 1998;49:367–372.
52. García-Labiano F, de Diego LF, Adánez J, Abad A, Gayán P. Reduction and oxidation kinetics of a copper-based oxygen carrier prepared by impregnation for chemical-looping combustion. *Ind Eng Chem Res*. 2004;43(26):8168–8177.
53. Nord LO, Bolland O. HRSG Design for integrated reforming combined cycle with CO_2 capture. *J Eng Gas Turbines Power*. 2011;133(1):011702.
54. Martelli E, Nord LO, Bolland O. Design criteria and optimization of heat recovery steam cycles for integrated reforming combined cycles with CO_2 capture. *Appl Energy*. 2012;92(5):255–268.
55. Darde A, Prabhakar R, Tranier J-P, Perrin N. Air separation and flue gas compression and purification units for oxy-coal combustion systems. *Energy Procedia*. 2009;1(1):527–534.

Manuscript received Aug. 10, 2012, and revision received Jan. 21, 2013.